

# Millisecond Pulsars as Probes of Mass Segregation in the Galactic Center

Julio Chanamé and Andrew Gould

*Department of Astronomy, The Ohio State University, Columbus, OH 43210, USA*

## ABSTRACT

We propose a simple test for the existence of a cluster of black hole remnants around Sgr A\* that is based on a small sample of any type of Galactic Center objects, provided they are substantially less massive than the black holes and constitute part of an old ( $\gtrsim 1$  Gyr) population. The test relies on the fact that, under the presence of such a cluster of heavy remnants and because of energy equipartition, lower mass objects would be expelled from the central regions and settle into a distribution very different than the cusp expected to be induced by the supermassive black hole alone. We show that with a sample of just 50 objects and using only their angular positions on the sky relative to Sgr A\* it is possible to clearly differentiate between a distribution consistent with the presence of the cluster of black holes and a power-law cusp distribution. We argue that millisecond pulsars might currently be the best candidate to perform this test, because of the large uncertainties involved in the age determination of less exotic objects. In addition, by measuring their first and second period derivatives, millisecond pulsars offer the rare opportunity of determining the complete phase space information of the objects. We show that this extra information improves the detection of mass segregation by about 30%.

*Subject headings:* black hole physics – Galaxy: center – Galaxy: kinematics and dynamics – pulsars: general – stellar dynamics

## 1. Introduction

Measurements of the proper motions, radial velocities, and even the accelerations of the closest resolvable stars at the Galactic Center (GC) have demonstrated the existence of a large concentration of mass inside their orbits, leading to the almost inevitable conclusion that a black hole with a mass of  $M_* \approx 3 \times 10^6 M_\odot$  lies at the center of the Galaxy, coinciding with the position of the GC radio source Sgr A\* (Eckart & Genzel 1997; Ghez et al. 1998;

Genzel et al. 2000; Ghez et al. 2000). The same improvements in near infrared (NIR) detection limits and in angular resolution that made this kind of work possible also show that the stars around the GC are part of a complex mixture of old and young populations, unlike the familiar, old Galactic bulge. Massive and young associations such as the Arches and Quintuplet clusters (Figer et al. 1999), HeI emission-line stars (Najarro et al. 1997) as well as Wolf-Rayet stars (Blum, Sellgren & Depoy 1995; Figer, McLean & Morris 1995), all represent clear evidence of episodes of star formation near the GC during the last  $10^7$  years (Krabbe et al. 1995).

In dynamical terms, a supermassive black hole is expected to produce a power law distribution,  $\rho(r) \sim r^{-\alpha}$ , of stars inside a cusp radius  $r_c$  on a timescale comparable to the relaxation timescale at  $r_c$ . Considering the case of a massive black hole in the center of globular clusters, Bahcall & Wolf (1976) predicted the formation of a  $r^{-7/4}$  cusp for a population of stars of equal masses. For a more realistic multi-mass stellar distribution it was found that each mass species forms a different cusp with power-law index in the range  $3/2 \leq \alpha \leq 7/4$  (Bahcall & Wolf 1977; Murphy et al. 1991), with the heavier stars more concentrated towards the center than the lighter ones. Evidence for this mass segregation in globular clusters exists in various forms: the slope of the stellar mass function (as derived from the luminosity function at different radii) continuously decreasing towards the cluster core, as found with the recent *Hubble Space Telescope (HST)* data on 47 Tuc (Howell et al. 2001; see also Sosin 1997); a more centrally concentrated radial distribution of objects such as pulsars (Phinney 1992) and blue stragglers (Coté, Richer & Fahlman 1991; Lanzerl et al. 1992; Layden et al. 1999; Marconi et al. 2001) as compared to subgiants and main sequence stars; and radial color gradients (Howell, Guhathakurta & Tan 2000). Measurement of the surface brightness profiles of the innermost parts of elliptical galaxies have shown that almost all of them, both “power-law” and “cuspy core” galaxies in the Nuker-type nomenclature, exhibit power law profiles all the way down to the  $\sim 0.^{\prime\prime}1$  resolution of *HST* (Faber et al. 1997; van der Marel 1999). Finally, in the context of the Galaxy and based on analysis of the star counts from recent NIR observations of the GC, Alexander (1999) concluded that the distribution of stars around Sgr A\* reveals the presence of a cusp with a power-law index consistent with the Bahcall & Wolf (1977) solution, arguing that a flat core is completely ruled out and that the apparent overdensity of faint stars in the inner  $\sim 0.05$  pc (the Sgr A\* cluster) is the tip of an underlying stellar cusp that smoothly rises throughout the inner  $10''$ . However, most of the stars so far detected in the NIR imaging of the GC are part of the youngest stellar population, and hence they are dynamically unrelaxed, i.e., they have not had enough time to achieve energy equipartition with the fainter, older stellar population that dominates the mass in the inner Galaxy. A detailed theoretical investigation of the distribution of stars of different masses around Sgr A\* constitutes an interesting problem

on its own and will be addressed in a future paper. Here we only want to note that the Bahcall & Wolf (1977) solution applies under assumptions of steady state as well as specific boundary conditions, both of which do not necessarily correspond to the conditions at the GC.

Recently, Miralda-Escudé & Gould (2000) predicted the existence of a cluster of black hole remnants around the GC. Integrating over the lifetime of the Galaxy and considering the rate of capture by Sgr A\*, they concluded that about 20,000 of these black holes have migrated by dynamical friction to the GC and should still be there, forming a compact cluster about 0.7 pc in radius ( $\sim 18''$  for a Galactocentric distance of 8 kpc). Chanamé, Gould, & Miralda-Escudé (2001) considered the possibility of detecting the cluster black holes by monitoring the pairs of images of background bulge stars that are lensed by Sgr A\*, looking for microlensing events induced by the surrounding black holes. They found that there should be about 2 such pairs for  $K < 21$  mag, and about 8 down to  $K=23$ . Then, if any of these pairs happens to be part of a high magnification event, the rate of microlensing events due to the cluster black holes, and hence the probability of detecting them, is reasonably high.

However, the simplest observable consequence of such a cluster of black holes is that, as a result of relaxation, any sufficiently old population of lower mass objects should have been expelled from the region occupied by the black hole cluster. This redistribution occurs on a timescale of about 1 Gyr (the relaxation timescale at a radius of 0.7 pc), so this effect should only be apparent in populations that are older than this (and substantially less massive than the black holes). Hence, the most direct way of testing for the presence of the cluster of black holes is to measure the distribution of the oldest possible population of objects and see whether they show this “core” or “hole” in their underlying distribution.

We show that if any such population is identified, then with only about 50 objects it is possible to differentiate between a distribution driven by the presence of a cluster of black holes and a regular power law distribution, by using only information on their angular positions on the sky.

Current age determinations of stars at the GC are still concentrated on the brightest objects, which are usually the most massive and youngest. Using  $K$ -band spectra, Blum, Sellgren & DePoy (1996) studied 19 bright GC stars (most of them supergiants and asymptotic giant branch stars), deriving relatively accurate ages for the youngest ones. These stars are not expected to show any effect from the cluster of black holes, both because their parent gas clouds do not fall into the lower-mass category and also because, since they are young, they have not been around long enough to be affected by the process of relaxation. Unfortunately, the uncertainties quoted by Blum et al. (1996) for the oldest stars in their sample

are so large that they could place only lower limits on their ages ( $\sim 440$  Myr). Until these uncertainties are greatly improved there will be no hope of using ordinary stars for testing the mass segregation induced by the cluster of black holes, because any contamination of the sample with young objects would undermine one's ability to differentiate between the two distributions. The oldest objects possible, as well as the most numerous, should be old, low-mass main sequence stars. Reaching these stars at the distance of the GC requires a sensitivity of at least  $K \sim 21$  (the main sequence turnoff being at  $K \sim 20$ ), which estimate takes into account an average of 3 magnitudes of extinction in the  $K$ -band (see the empirical luminosity function of the GC derived in Chanamé et al. 2001). Moreover, at  $K \sim 21$  one expects  $\sim 400$  arcsec $^{-2}$  stars of similar magnitude and brighter, so that milliarcsec resolution would be required. Such deep, high-resolution observations are beyond current capabilities, but may be achievable with improvements in adaptive optics, or with NGST.

A very interesting alternative are millisecond (ms) pulsars. Being neutron stars, these are lighter than the remnant black holes and, furthermore, constitute an old population of objects as estimated by their spindown timescale  $P/(2\dot{P})$ , typically several Gyr for ms pulsars,  $\log(P_{\text{sec}}) \lesssim -2$  (Taylor, Manchester, & Lyne 1993). Since ms pulsars would be selected on an observable directly related to their ages, the contamination by young objects would be extremely low. Moreover, pulsars offer the possibility of adding more information than just the usual sky positions and proper motions. Measurements of the first and second period derivatives of a pulsar orbiting the GC yield, up to a two-fold ambiguity, its position and velocity along the line of sight, hence completing the entire 6-dimensional phase-space information. Certainly, both  $\dot{P}$  and  $\ddot{P}$  have contributions that are intrinsic to the pulsar. However, for ms pulsars,  $(\dot{P}/P)_{\text{int}} \lesssim 10^{-17} \text{ s}^{-1}$ , is more than two orders of magnitude smaller than the variation induced by the acceleration towards Sgr A\* over the region of interest,  $(\dot{P}/P)_{\text{GC}} = (GM_*c^{-1})/(0.7\text{pc})^2 \approx 3 \times 10^{-15} \text{ s}^{-1}$  (note that, 10 times farther away than this, i.e., 3 arcmin in projection from the GC, the intrinsic  $\dot{P}/P$  already becomes important). Similarly,  $(\ddot{P}/P)_{\text{int}} \sim 10^{-31} \text{ s}^{-2}$  (Phinney 1993), again, much smaller than the contribution from the Sgr A\* potential,  $(\ddot{P}/P)_{\text{GC}} = (\dot{P}/P)_{\text{GC}}/\tau_{\text{orb}} \approx 2 \times 10^{-26} \text{ s}^{-2}$ , where  $\tau_{\text{orb}}$  is the orbital timescale of the pulsar around the GC. Hence, the intrinsic period derivatives of the pulsars do not represent a limitation for our purposes. Nevertheless, because of the crowded GC environment passing stars can produce effects that mimic  $\ddot{P}$ , as we discuss in § 2.2. We find that the extra information obtained by measuring the position and velocity of the pulsars along the line of sight does indeed improve one's ability to differentiate between different underlying pulsar distributions as compared with using only the sky positions. However, the improvement is modest, only  $\sim 30\%$ .

A problem with using pulsars as probes of mass segregation arises because the high density of free electrons in the central regions of the Galaxy strongly scatters radio waves,

broadening the pulsar pulses by extraordinary amounts and hence making difficult their detection by periodicity searches (see Cordes & Lazio 1997). As a result, today there are no known pulsars closer than  $1^\circ$  to the GC. Nevertheless, the degree of pulse broadening is strongly frequency dependent ( $\Delta t \sim \nu^{-4}$ ), and most pulsar searches have been made at frequencies like 0.4 GHz, where this effect is known to be large. Using a model for the distribution of free electrons in the Galaxy (Taylor & Cordes 1993), Johnston et al. (1995) carried a search for pulsars near the GC at 1.5 GHz, a frequency specifically chosen so as to minimize the broadening of the pulses ( $\Delta t(0.4 \text{ GHz})/\Delta t(1.5 \text{ GHz}) = (1.5/0.4)^4 \approx 200$ ). None were found, suggesting that there is substantial scattering in the GC that is not taken into account by the Taylor & Cordes (1993) electron density model. It is clear then, that future searches for pulsars near the GC must be done at even higher frequencies, such as 5 or 15 GHz, where the pulse broadening is smaller than at 1.5 GHz by factors of  $10^2$  and  $10^4$ , respectively. Improvements in sensitivity are also needed for such a search, both in order to have more potential targets (the observed local luminosity function of pulsars scales as  $N(L) \sim L^{-1}$ ) and because the pulsar spectral energy distribution decreases with frequency ( $F_\nu \sim \nu^{-1.4}$ ). The planned Square Kilometer Array (SKA), with about two orders of magnitude increased sensitivity over existing facilities, is the indicated choice for these searches. Another possibility is to conduct imaging rather than periodicity surveys. These may be far more successful since angular broadening is not as severe as pulse broadening (see Cordes & Lazio 1997).

In § 2 we present the input density models used to simulate data, describe our maximum likelihood approach, and show how ms pulsars improve the results as compared to less exotic objects. In § 3 we present the results and discuss them, summarizing our conclusions.

## 2. Input Density Profile and Likelihood Analysis

### 2.1. The General Case

Lower mass objects expelled from the inner GC region will show in their distribution an overdensity at some radius  $r_0$  of the order of the radius of the black hole cluster, producing something that would resemble a “core” or “hole” around the GC. We model this with the family of functions

$$\nu(r) = C \left( \frac{1}{r^2} + \frac{1}{r_0^2} \right)^{-\alpha/2} \left( r^2 + r_0^2 \right)^{-\beta/2}, \quad (1)$$

and study combinations of  $(r_0, \alpha, \beta)$ . The larger the value of  $\alpha$  the more evident the core/hole

around the GC, and the larger the value of  $\beta$  the narrower the distribution around  $r_0$ . The normalization constant is chosen such that the volume integral of  $\nu(r)$  is equal to the size of the sample. Note that fixing  $\alpha$  equal to zero and using a very small  $r_0$ , yields a power-law density profile,  $\nu(r) \sim r^{-\beta}$ . Figure 1 illustrates the differences between a distribution for the tracer population that is consistent with a black hole cluster around the GC, and a power law distribution. Figure 1 shows the model with the biggest hole considered in this work.

We first describe the simplest case, in which the only information used is the pulsar positions on the plane of the sky. Later more information will be included. Given a set of data  $\{\boldsymbol{\theta}_k; k = 1 \dots N\}$  on  $N$  objects (where  $\boldsymbol{\theta}_k = (\theta_k^x, \theta_k^y)$  represents the angular position of the  $k$ -th object) that follow some unknown underlying parent distribution, denoted as  $(r_0^*, \alpha^*, \beta^*)$ , we want:

- First, to compare the likelihoods that all those coordinates are coming from: (a) a distribution consistent with a cluster of black holes being at the GC, and (b) a power-law distribution, as would be expected in the absence of a black hole cluster.
- Second, to know how accurately the underlying parameters  $(r_0^*, \alpha^*, \beta^*)$  can be recovered from the data.

To achieve this, we choose the input model  $(r_0^*, \alpha^*, \beta^*)$  consistent with the presence of a cluster of black holes (i.e., with a core/hole in the distribution around the GC) and generate random positions for  $N$  objects. This data set is then given to a routine that, using the downhill SIMPLEX method for minimization in multidimensions (Press et al. 1992), finds the parameters of the distribution  $(r_0, \alpha, \beta)$  that maximize the likelihood function, as given by

$$\ln \mathcal{L} = \sum_{k=1}^N \ln \mathcal{P}(\{\boldsymbol{\theta}_k\} | r_0, \alpha, \beta) = \sum_{k=1}^N \ln \int_{-\infty}^{\infty} dz \nu(r_k) dx_k dy_k , \quad (2)$$

where  $\mathcal{P}(\{\boldsymbol{\theta}_k\} | r_0, \alpha, \beta)$  denotes the probability of the occurrence of the  $k$ -th data point given the model distribution  $(r_0, \alpha, \beta)$  being tested,  $r_k = \sqrt{x_k^2 + y_k^2 + z^2}$ , and the integral over  $z$  reflects our (in general) ignorance of the position of any given object along the line of sight. Equation (2) makes immediately obvious that, in order to transform from the observable quantities  $\{\boldsymbol{\theta}_k\}$  to actual lengths, one needs to assume a distance to the GC,  $D_{GC}$ . Throughout this paper we adopt  $D_{GC} = 8$  kpc. We discuss the effects of the uncertainty in this parameter in §3. The experiment is repeated several times (each time using a new set of data) for the two distributions that we wish to compare. When testing for a power-law

distribution, we fix the value of  $\alpha$  to zero and of  $r_0$  to a very small value, 0.1. Computing the statistics of the outcome of all these experiments we finally obtain:

- the difference between the mean values of  $\ln\mathcal{L}$  for the two competing distributions, which tells whether or not it is possible to differentiate between them and with how much confidence.
- the mean and variances of each of the fitted parameters  $(r_0, \alpha, \beta)$ , which tells how well the input model  $(r_0^*, \alpha^*, \beta^*)$  can be recovered from the data.

Equation (2) illustrates the simplest case, in which the available information reduces to just the two-dimensional positions of the objects on the sky. It is still possible to include two-dimensional velocity information by measurement of the proper motions,  $\boldsymbol{\mu}_k = (\mu_k^x, \mu_k^y)$ , and that would be, for a general class of objects, all the information that one could possibly add.

## 2.2. Millisecond Pulsars

However, if the objects being used for this test are ms pulsars, then it is possible to add even more information to the likelihood, the position and velocity of the pulsars along the line of sight ( $z$  and  $v_z$ ). This is accomplished as follows. First, the line of sight acceleration,  $a_z$ , can be derived by measuring the first time derivative of the pulsar's period,  $\dot{P}$ , as has been successfully done for several pulsars in globular clusters (Phinney 1993; Robinson et al. 1995; Freire et al. 2001). This acceleration can in turn be related to the actual pulsar position with respect to Sgr A\* by

$$\frac{GM}{b^2} \sin^2 \eta \cos \eta = -a_z = -\frac{\dot{P}}{P} c, \quad (3)$$

where  $M$  is the mass interior to the pulsar radius (essentially the mass of Sgr A\*),  $b$  is the impact parameter with respect to Sgr A\*, and  $\eta$  is the angle defined by the observer, the pulsar, and Sgr A\*. It is necessary to stress here that this can be safely done only in the case of ms pulsars, for which the contribution to  $\dot{P}$  due to intrinsic pulsar spindown is negligible with respect to the contribution due to acceleration towards Sgr A\* over the region of interest. The function  $\sin^2 \eta \cos \eta$  is double valued in the interval  $[0, \pi]$ , so there are two possible values for the position along the line of sight,  $z = b \cot \eta$ . Both degenerate solutions must enter in the calculation, since they represent a fundamental uncertainty that can not

be broken with the information considered here. The measurement of  $\eta$  together with the position on the sky gives complete spatial information, and the distance from Sgr A\* is simply  $r = b \csc \eta$ . Second, two components of the velocity,  $\mathbf{v}_\perp$ , are given by measurement of the pulsar's proper motion. The third component of the velocity can be determined by measuring the pulsar jerk,  $\dot{a}_z$ , from measurement of  $\ddot{P}/P$ . Specifically,

$$v_z = \frac{b}{GM \sin \eta (3 \cos^2 \eta - 1)} \left( \frac{\dot{a}_z b^2}{\sin^2 \eta} + 3a_z \mathbf{b} \cdot \mathbf{v}_\perp \right), \quad (4)$$

where the expression has been written in terms of observables, except for the two-fold discretely degenerate parameter  $\eta$ . When using millisecond pulsars, then, the probability that goes into equation (2) must be the sum of the individual probabilities for each of the two degenerate pulsar positions, i.e.,  $\mathcal{P}(\{\boldsymbol{\theta}_k, \boldsymbol{\mu}_k, \dot{P}_k, \ddot{P}_k\} | r_0, \alpha, \beta) = \mathcal{P}_{k1} + \mathcal{P}_{k2}$ , where

$$\mathcal{P}_{ki} = \nu(r_{ki}) \frac{1}{(2\pi\sigma_{ki}^2)^{3/2}} \exp\left[-(v_x^2 + v_y^2 + v_{zi}^2)/2\sigma_i^2\right]_k d^6V_k^i; \quad i = 1, 2. \quad (5)$$

Here  $\sigma_{ki} = \sigma(r_{ki})$  is the one-dimensional velocity dispersion at  $r_{ki}$ , computed assuming an isotropic velocity distribution for the model  $(r_0, \alpha, \beta)$  (Binney & Tremaine 1987), and  $d^6V_k^i = dx_k dy_k dz_k^i dv_{xk} dv_{yk} dv_{zk}$  is the six-dimensional phase-space volume element centered on  $\{\mathbf{x}_i, \mathbf{v}_i\}_k$ . Due to the transformation from observables to actual positions and velocities, this volume element is not the same for the two degenerate positions. Hence, while the part  $dx_k dy_k dv_{xk} dv_{yk}$  can be simply factored-out from the expression for the probability (because it is the same for both  $i=1,2$ ), one must replace  $dz_k^i dv_{zk} \rightarrow J_k^i d\dot{P}_k d\ddot{P}_k$ , where  $J_k^i$  is the Jacobian of the transformation  $(z, v_z)_k \rightarrow (\dot{P}, \ddot{P})_k$ . Only now can one factor out the observable part of the volume element, keeping the factors  $J_k^i$ , which need to be computed each time for  $\mathcal{P}_{k1}$  and  $\mathcal{P}_{k2}$ .

The time derivatives of the pulsar's period,  $\dot{P}$  and  $\ddot{P}$ , are currently measured to great precision: for a 10 ms pulsar and over a time baseline of 3 years, Phinney (1993) quotes a measurement accuracy of  $\dot{P}/P \approx 3 \times 10^{-20} \text{ s}^{-1}$ , and  $\ddot{P}/P \approx 10^{-27} \text{ s}^{-2}$ . Recall that, as discussed in § 1, the pulsar's intrinsic period derivatives are not a source of uncertainty for our purposes. However, a passing star can introduce uncertainties, though these are only important to the determination of the pulsar's jerk. The effect of a passing star of mass  $m_i$  on  $\ddot{P}$  can be estimated computing the product of the induced acceleration,  $G m_i/d^2$ , and  $(\sqrt{3} \sigma_{stars}/d)$ , where  $\sigma_{stars}$  is the one-dimensional velocity dispersion of the stars at the pulsar's position and  $d$  is the star-pulsar distance, and asking what this distance would have to be in order for the passing star to produce an effect as large as that due to Sgr A\*,  $(\ddot{P}/P)_{GC}$ . We obtain,  $d \simeq (4/11)^{1/6} (m_i/M_*)^{1/3} r$ , where  $r$  is the distance to Sgr A\* and the

numerical factor in front comes from assuming a stellar density profile proportional to  $r^{-7/4}$ . Finally, the probability of such a close encounter with a star of this particular type (mass  $m_i$ ) goes as  $n_i d^3$ , where  $n_i$  is the number density of stars of mass  $m_i$ . Summing over all the types of stars, this probability then scales as  $\rho r^3$ , where  $\rho(r)$  is the total stellar mass density, as given by equation (3) in Miralda-Escudé & Gould (2000). Specifically, we obtain  $(4\pi/3)(12/11)^{1/2}\rho(r)r^3/M_* \approx 0.13$ , i.e., there is a modest chance that a close encounter affects the pulsar’s jerk by a large factor. A similar argument shows that the probability that a passing star will significantly affect  $\dot{P}$  is only  $\sim 10^{-4}$  (see also Phinney 1993).

### 3. Results and Discussion

We run simulations consisting of 400 experiments, where an experiment includes both the generation of the data and fitting them to either one of the competing distributions, as described in §2.1. In each experiment we generate data for  $N = 50$  objects. Table 1 shows the results of simulations for four different input models, labeled by the corresponding combination of  $(r_0^*, \alpha^*, \beta^*)$ . The models presented in Table 1 are chosen to have varying sizes of the inner core/hole in the distribution of stars, with the first one being the most evident (see Fig. 1), peaking beyond the radius predicted for the cluster of black holes ( $\sim 0.7$  pc, Miralda-Escudé & Gould 2000). Then, by using smaller values for  $r_0^*$  and  $\alpha^*$ , this hole is made progressively smaller in the next two models, until in the third model the peak is at about half the black hole cluster radius. The third model has a tail at large radii that falls slower than in the first two models (i.e., smaller  $\beta^*$ ), making the distribution less concentrated around the peak, and hence even more difficult to differentiate from a simple power law. The fourth model has  $\alpha=0.0$ , so that a core, rather than a hole, is set at the origin. Each entry in the table, which we denote  $\Delta \ln \mathcal{L}$ , is the difference between the mean values of  $\ln \mathcal{L}$  when fitting for a distribution consistent with the presence of a cluster of black holes and when fitting for a power law distribution, *in that order*. For each input model we compute  $\Delta \ln \mathcal{L}$  in four different cases (columns 2 to 5 in Table 1), each one providing an increasing amount of information to the likelihood calculation. Note that columns 3 and 4 do not represent realistic data sets (since they imply knowledge of the 3 dimensional position and velocity of the star without any ambiguity), but they are helpful in understanding both what kind of information is the most valuable (i.e., that information that contributes the most to  $\ln \mathcal{L}$ ), and to what degree the ambiguity in the  $z$  position degrades the likelihood.

Table 1.  $\Delta \ln \mathcal{L}$

input model $(r_0^*, \alpha^*, \beta^*)$	$(x, y)$	$(x, y, z_1)$	$(\mathbf{x}_1, \mathbf{v}_1)$	millisecond pulsars
(1.0, 2.0, 4.0)	22.3	27.1	29.8	28.1
(0.5, 1.0, 4.0)	16.2	20.0	22.2	20.9
(0.3, 0.5, 3.3)	4.7	5.8	6.4	6.0
(1.0, 0.0, 4.0)	18.6	22.5	24.8	23.0

The first column of  $\Delta \ln \mathcal{L}$  values (second column in Table 1), labeled  $(x, y)$ , represents the simplest case (see eq. 2), in which the only information available for the test is the pulsar positions on the plane of the sky. As expected, the larger the hole at the center of the distribution, the larger the value of  $\Delta \ln \mathcal{L}$ , i.e., the easier it is to distinguish between the two competing models. The conclusion from this first set of experiments is that with the angular positions of only 50 GC objects one can easily tell if their distribution is consistent or not with a cluster of black holes at the GC, *provided that all the objects in the sample are old enough ( $\gtrsim 1$  Gyr) to have achieved relaxation.*

Millisecond pulsars have the advantage that they do not present any age related problem, and furthermore, as discussed in § 2.2, they offer the unique opportunity to obtain the complete phase space coordinates on the individual objects, so that all the space and velocity information can be included in the likelihood calculation. In the fifth (last) column of Table 1 we present the results of experiments that simulate the use of ms pulsars, i.e., they assume knowledge of all six phase space coordinates and take into account the two-fold ambiguity described in § 2.2. One can see that  $\Delta \ln \mathcal{L}$  grows in all four input models by about 30% of the value obtained when using only the positions on the sky. We conclude then that this extra information coming from the use of ms pulsars does not improve the confidence in the results by a large factor: it has the same effect as adding  $\sim 15$  objects to the original sample and performing the test using just the angular positions on the sky. Hence, the real advantage of the use of ms pulsars is the certainty that one is using a sufficiently old population, so that young, unrelaxed objects do not contaminate the sample.

With the aim of gaining a better understanding on the nature of the information that is enhancing and/or degrading the value of  $\Delta \ln \mathcal{L}$ , we perform two extra sets of experiments under the (unrealistic) supposition that no ambiguity in the determination of the three-dimensional position and velocity of the pulsars is present at all. First, we suppose that the three dimensional position,  $(x, y, z_1)$ , can be known without ambiguity, and second, we suppose that the three dimensional velocity,  $(v_x, v_y, v_{z1})$ , can also be known with no ambiguity. The results of these extra experiments are given in the third and fourth columns of Table 1, respectively. Comparison between the fourth and fifth columns immediately shows that the two-fold ambiguity in the actual determination of  $z$  and  $v_z$  hardly degrades  $\Delta \ln \mathcal{L}$  at all relative to complete phase information. Instead, by comparing the second and third columns one realizes that by far the largest improvement comes from knowledge of the 3-d position in space with respect to Sgr A\*. Finally, adding the velocity information (compare the third and fourth columns in Table 1) makes only a marginal improvement. Recall here, from the discussion in § 2.2, that the line-of-sight velocity of the pulsars are the most uncertain measurements of those considered here, so, happily for our purposes, they are at the same time the least useful. That is, the spatial position of the objects with respect

to Sgr A\* is the most important ingredient in this test, and, fortunately, it happens to be the easiest to determine.

Finally, what are the effects of an uncertainty in the value of  $D_{GC}$ ? The distance to the GC enters our calculation in two places: through the positions and velocities that are simulated, and through  $M_*$ , the adopted total mass of the supermassive black hole. The latter scales as  $\propto D_{GC}^3$  if it is determined from measurements of the proper motions of the stars close to Sgr A\*. Hence, our likelihood analysis should not be affected when using only angular positions and proper motions. The coordinates along the line of sight ( $z$  and  $v_z$ ), however, have a non trivial dependence on  $D_{GC}$ , so it is not easy to predict the effect of varying  $D_{GC}$  in the case where we use all phase space information. In order to quantify these we compute  $\Delta \ln \mathcal{L}$  for different values of  $D_{GC}$ . We indeed find that when using only angular positions, the value of  $\Delta \ln \mathcal{L}$  remains exactly the same regardless of the value of  $D_{GC}$ . This is not the case when using all the phase space information, for which a 10% increase in the adopted Galactocentric distance has the effect of changing the value of  $\Delta \ln \mathcal{L}$  by a small amount (about 2% of tabulated values), hence introducing no effective change in one's ability to distinguish the two different distributions. When performing the test with only the angular positions as inputs (as in the second column in Table 1), the recovered (fitted) *angular size* of the hole in the distribution,  $r_0/D_{GC}$ , remains constant, as expected when using just angular measurements. However, when including all the phase space information (as in the last column in Table 1) the hole's angular size increases approximately linearly with  $D_{GC}$ . The fitted angles  $\alpha$  and  $\beta$ , as well as the uncertainties in the three parameters, do not change when varying  $D_{GC}$ . We conclude that the uncertainty in the Galactocentric distance does not affect the reliability of the test in determining the underlying distribution of the tracers.

In summary:

- the simple analysis of the angular distribution of any old population of objects that have achieved relaxation around the GC constitutes a powerful probe of mass segregation in the GC, in particular as a test for the existence of a cluster of stellar mass black holes around Sgr A\*.
- a sample of only 50 objects is enough to obtain reliable results, and the only measurements needed are their positions relative to Sgr A\*. Velocity information does not contribute appreciably to the results.
- provided it is older than  $\sim 1$  Gyr, any population of objects with masses substantially lower than that of the black holes is in principle equally well fitted to be used in the test. Being intrinsically a very old population, ms pulsars might currently be the most

promising candidate, because the determination of the ages of normal stars at the GC is too uncertain. However, improvements in search techniques, as well as in sensitivity at radio wavelengths, are needed to find pulsars in the difficult GC environment. Future radio facilities such as the planned SKA will probably be required to carry out the high frequency pulsar searches ( $\nu \gtrsim 5$  GHz) and/or imaging surveys needed to find pulsars near the GC.

- the use of ms pulsars provides the opportunity of determining the complete phase space information of the objects, improving the results by about 30%. The improvement comes primarily from the addition of information on the position  $z$  of the pulsars along the line of sight with respect to Sgr A\*, i.e., from the measurement of the pulsar's first period derivative (§ 2.2). Measurement of the second period derivative leads to knowledge of the velocity along the line of sight, but there is little to be gained from this.

Work by AG was supported in part by grant AST 97-27520 from the NSF.

## REFERENCES

Alexander, T. 1999, ApJ, 527, 835

Bahcall, J.N., & Wolf, R.A. 1976, ApJ, 209, 214

Bahcall, J.N., & Wolf, R.A. 1977, ApJ, 216, 883

Binney, J., & Tremaine, S. 1987, Galactic Dynamics (Princeton: Princeton University Press) 210

Blum, R.D., Sellgren, K., & DePoy, D.L. 1995, ApJ, 440, L17

Blum, R.D., Sellgren, K., & DePoy, D.L. 1996, AJ, 112, 1988

Cordes, J.M. & Lazio, T.J.W. 1997, ApJ, 475, 557

Coté, P., Richer, H.B., & Fahlman, G.G. 1991, AJ, 102, 1358

Chanamé, J., Gould, A., & Miralda-Escudé, J. 2001, ApJ, 563, 793

Eckart, A., & Genzel, R. 1997, MNRAS, 284, 576

Faber, S.M., Tremaine, S., Ajhar, E.A., Byun, Y., Dressler, A., Gebhardt, K., Grillmair, C., Kormendy, J., Lauer, T.R., & Richstone, D. 1997, AJ, 114, 1771

Figer, D., McLean, I., Morris, M. 1995, ApJ, 447, L29

Figer, D., Kim, S.S., Morris, M., Serabyn, E., Rich, R.M., McLean, I.S. 1999, ApJ, 525, 750

Freire, P.C., Camilo, F., Lorimer, D.R., Lyne, A.G., Manchester, R.N., & D'Amico, N. 2001, MNRAS, 326, 901

Genzel, R., Pichon, C., Eckart, A., Gerhard, O.E., & Ott, T. 2000, MNRAS, 317, 348

Ghez, A.M., Klein, B.L., Morris, M., & Becklin, E.E. 1998, ApJ, 509, 678

Ghez, A.M., Morris, M., Becklin, E.E., Tanner, A., & Kremenek, T. 2000, Nature, 407, 349

Howell, J.H., Guhathakurta, P., & Tan, A. 2000, AJ, 119, 1259

Howell, J.H., Warren, J.A., Guhathakurta, P., Gilliland, R.L., Albrow, M.D., Sarajedini, A., Brown, T.M., Charbonneau, D., Burrows, A.S., Cochran, W.D., Baliber, N., Edmonds, P.D., Frandsen, S., Bruntt, H., Lin, D.N.C., Vogt, S.S., Choi, P., Marcy, G.W., Mayor, M., Naef, D., Milone, E.F., Stagg, C.R., Williams, M.D., Sigurdsson, S., & VandenBerg, D.A. 2001, American Astronomical Society Meeting 198, 9505

Johnston, S., Walker, M.A., van Kerkwijk, M.H., Lyne, A.G., & D'Amico, N. 1995, MNRAS, 274, L43

Krabbe, A., Genzel, R., Eckart, A., Najarro, F., Lutz, D., Cameron, M., Kroker, H., Tacconi-Garman, L.E., Thatte, N., Weitzel, L., Drapatz, S., Geballe, T., Sternberg, A., & Kudritzki, R. 1995, ApJ, 447, L95

Lauzeral, C., Ortolani, S., Auriere, M., & Melnick, J. 1992, A&A, 262, 63

Layden, A.C., Ritter, L.A., Welch, D.L., & Webb, T.M.A. 1999, AJ, 117, 1313

Marconi, G., Andreuzzi, G., Pulone, L., Cassisi, S., Testa, V., & Buonanno, R. 2001, astro-ph/0111083

Miralda-Escudé, J., & Gould, A. 2000, ApJ, 545, 847

Murphy, B.W., Cohn, H.N., & Durisen, R.H. 1991, ApJ, 370, 60

Najarro, F., Krabbe, A., Genzel, R., Lutz, D., Kudritzki, R.P., & Hillier, D.J. 1997, A&A, 325, 700

Phinney, E.S. 1993, in ASP Conf. Ser. 50, Structure and Dynamics of Globular Clusters, ed. S. G. Djorgovski & G. Meylan (San Francisco: ASP), 141

Press, W.H., Teukolsky, S.A., Vetterling, W.T., Flannery, B.P. 1992, Numerical Recipes, Cambridge University Press

Robinson, C., Lyne, A.G., Manchester, R.N., Bailes, M., D'Amico, N., & Johnston, S. 1995, MNRAS, 274, 547

Sosin, C. 1997, AJ, 114, 1517

Taylor, J.H., Manchester, R.N., & Lyne, A.G. 1993, ApJS, 88, 529

Taylor, J.H., & Cordes, J.M. 1993, ApJ, 411, 674

van der Marel, R.P. 1999, AJ, 117, 744

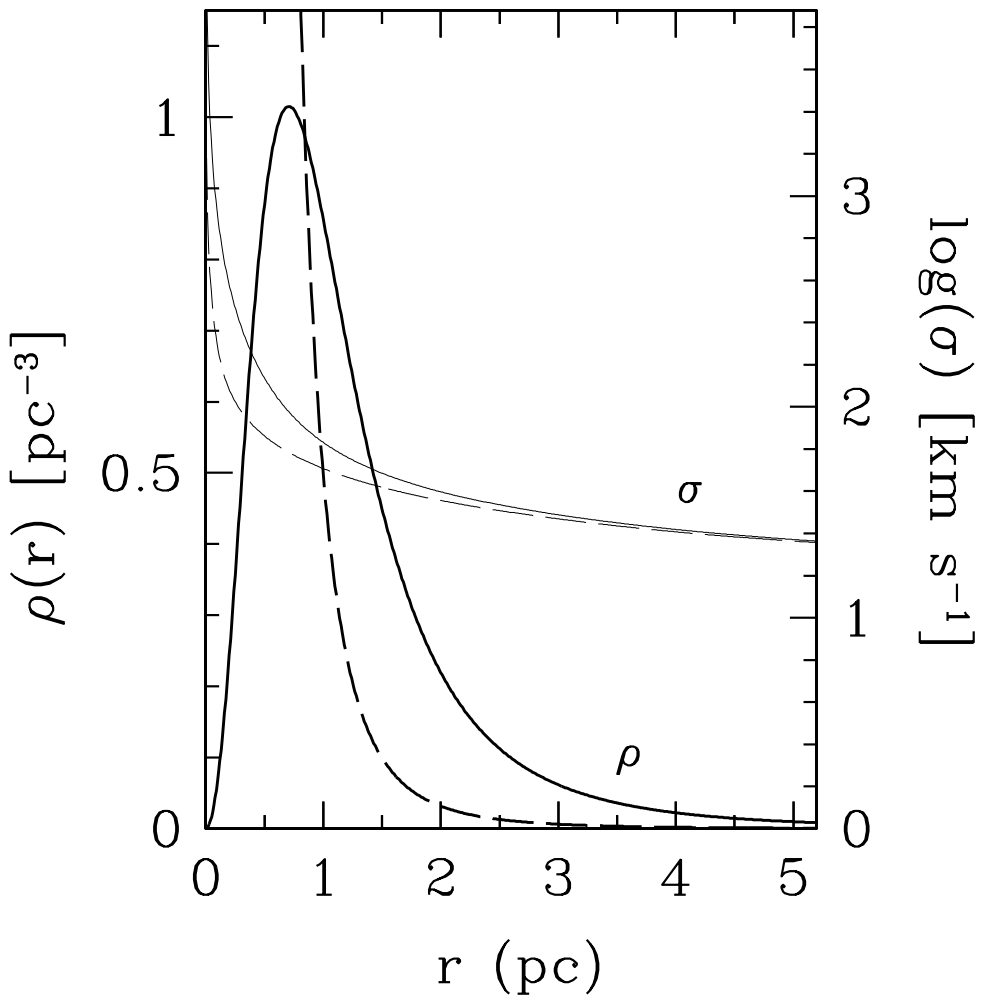


Fig. 1.— Illustration of the two competing distributions. Solid lines correspond to a distribution consistent with a cluster of black holes around the GC, with parameters  $(r_0, \alpha, \beta) = (1.0, 2.0, 4.0)$ , and dashed lines correspond to a power law distribution with parameters  $(r_0, \alpha, \beta) = (0.1, 0.0, 4.0)$ .